Published online 11 January 2011 *Nucleic Acids Research, 2011, Vol. 39, No. 9* ***3939–3948***
doi:10.1093/nar/gkq1347

Triplex inducer-directed self-assembly of single-walled carbon nanotubes: a triplex DNA-based approach for controlled manipulation of nanostructures

Chao Zhao[1,2], Konggang Qu[1,2], Can Xu[1,2], Jinsong Ren[1] and Xiaogang Qu[1,*]

[1]Laboratory of Chemical Biology, Division of Biological Inorganic Chemistry, State Key Laboratory of Rare Earth Resource Utilization, Changchun Institute of Applied Chemistry and [2]Graduate School of the Chinese Academy of Sciences, Chinese Academy of Sciences, Changchun, Jilin 130022, China

Received October 4, 2010; Revised December 20, 2010; Accepted December 22, 2010

ABSTRACT

As a promising strategy for artificially control of gene expression, reversible assembly of nanomaterials and DNA nanomachine, DNA triplex formation has received much attention. Carbon nanotubes as gene and drug delivery vector or as 'building blocks' in nano/microelectronic devices have been successfully explored. Therefore, studies on triplex DNA-based carbon nanotube hybrid materials are important for development of smart nanomaterials and for gene therapy. In this report, a small molecule directed single-walled carbon nanotubes (SWNTs) self-assembly assay has been developed by disproportionation of SWNTs–$dT_{22}\cdot dA_{22}$ duplex into triplex $dT_{22}\cdot dA_{22}\cdot dT_{22}$ and dA_{22} by a triplex formation inducer, coralyne. This has been studied by circular dichroism, light scattering (LS) spectroscopy, scanning electron microscopy (SEM), atomic force microscopy (AFM), electrophoretic mobility shift assay and supported by using DNA random sequence. In contrast, SWNTs do not aggregate under the same experimental conditions when the small molecules used can not induce $dT_{22}\cdot dA_{22}\cdot dT_{22}$ triplex formation. Therefore, this novel small molecule-directed SWNTs self-assembly assay has also been used for screening of triplex inducers in our studies.

INTRODUCTION

As the leading nanodevice candidate, single-walled carbon nanotubes (SWNTs) have great potential applications in electronics, optics, mechanics, thermal transportation and biosensing (1–4). The use of carbon nanotubes as 'building blocks' in nano/microelectronic devices could revolutionize the electronic industry in the same way that the microchips have revolutionized the computer industry. Individual SWNTs have been utilized to realize molecular-scale electronic devices such as single-electron (5) and field-effect transistors (6). Several SWNTs-based devices have been successfully integrated into logic circuits (7) and transistor arrays (8). A key challenge for the application of SWNTs is how to assemble them into desired large architectures, that has attracted much attention. Self-assembly based on molecular recognition establishes a promising approach for designing complex architectures from SWNTs that excludes the need for precise nanofabrication and mechanical manipulations (9). Biological molecules, such as DNA and RNA, possess highly specific and precise molecular recognition capability (10–12) that can be evolved through genetic engineering and can exert rational control over assembly and hierarchical pattern formation at a molecular scale. Integration of such unique capabilities of oligonucleotides with novel nanomaterials can offer many opportunities for bottom-up fabrication, including hierarchical assembly of 2D and 3D functional nanoarchitectures, molecular electronic and optoelectronic devices and molecular sensors (13).

Recently, functionalization of SWNTs with biomolecules has drawn much attention in nanotechnology because of their potential applications in molecular electronics, field-emission devices, biomedical engineering and biosensors (14). Several studies are particularly devoted to the generation of SWNTs–DNA complexes via two major routes: covalent construction (15,16) and non-covalent association (17,18). More recently, self-assembly strategies based on the biorecognition capability of single-stranded DNA (ssDNA) have been proposed (19–22). However,

*To whom correspondence should be addressed. Tel: +86 431 8526 2656; Fax: +86 431 8526 2656; Email: xqu@ciac.jl.cn

most of the multicomponent structures fabricated by self-assembling of multiple carbon nanotubes are directed by DNA hybridization.

Triple-helix DNA (triplex) is a well-documented structure in biology that is formed by the association of a target duplex and a homopyrimidinic 'triplex-forming oligonucleotide' (23). As a possible means to artificially control gene expression (24–27), reversible assembly of nanomaterials (28,29) and DNA nanomachine (30–34), DNA triplex formation has received much attention. However, for most triplex sequences the binding of the third strand (i.e. Hoogsteen strand) is considerably less stable than the Watson–Crick duplex (35). Previous studies have indicated that some small molecules with planar structures can facilitate triplex formation and stabilize triplex. Coralyne, a small crescent-shape molecule, can bind strongly to single-stranded homoadenine-containing nucleic acids. Our previous studies have shown that coralyne can induce poly(rA) tail in the 3′-end of mRNA self-structured that has a melting temperature of 60°C (36). Polak and Hud have demonstrated that coralyne can cause the strands of poly(dA)•poly(dT) to repartition into an equimolar amount of triplex poly(dT)•poly(dA)•poly(dT) and poly(dA) (37,38). Therefore, a small molecule that can bind to these kinds of DNA and/or RNA and trigger the formation of non-Watson–Crick secondary structures would be useful not only for design of potential new therapeutics but also for generating dynamic nucleic acid nanostructures.

In this article, we demonstrate that small molecule coralyne-induced triplex formation can direct SWNTs assembly through disproportionation of SWNTs–dT_{22}•dA_{22} duplex into triplex dT_{22}•dA_{22}•dT_{22} and dA_{22}. This novel small molecule-directed SWNTs self-assembly assay has also been used for screening of triplex inducers in our studies. To the best of our knowledge, this is the first example to use SWNTs assambly to detect triplex structure formation.

MATERIALS AND METHODS

Materials

SWNTs (φ = 1.1 nm, purity > 90%) were purchased from Aldrich (St Louis, MO, USA), purified as described previously by sonicating SWNTs in a 3:1 v/v solution of concentrated sulfuric acid (98%) and concentrated nitric acid (70%) for 10 h at 35–40°C, and washed with water, leaving an open hole in the tube side and functionalizing the open end of SWNTs with carboxyl group (39–43).

DNA oligomers, dT_{22}, its corresponding complementary strand dA_{22}, the amino-end-functionalized $(dT)_{22}$ [5′-$(dT)_{22}$-3′-NH_2], and the control DNA (5′-CCA ACC CCC CAG AAA GAA-3′) were purchased from Sangon (Shanghai, China) and used without further purification. 1-Ethyl-3-(3-dimethyl aminopropyl) carbodiimide hydrochloride (EDC) was purchased from BBI (Bio Basic Inc.), Sulfo-N-hydroxy succinimide (Sulfo-NHS) was purchased from Pierce. 2-[N-morpholino] ethanesulfonic acid (MES), sodium dodecyl sulfate (SDS), Triton X-100 and coralyne chloride were purchased from Sigma and used as received. Coralyne chloride was dissolved in water and its concentration was determined by UV–Vis spectrometry using the extinction coefficient of $\varepsilon_{420\,nm} = 14500\,M^{-1}\,cm^{-1}$. The others are of analytical or biochemical grade reagents.

Preparation of SWNTs-$(dT)_{22}$ conjugates

A 0.5 mg portion of oxidized, shortened SWNTs was suspended in 5 ml 100 mM MES buffer (pH 6.0) containing 0.2% Triton X-100 and sonicated for 1 h at room temperature. Add 20 mM EDC, 20 mM sulfo-NHS (set to pH 6.0) and stirred for another 1 h. Following the activation step, the pH was raised to 8.5, and the amino-modified $(dT)_{22}$ was added to a final concentration of 2 μM. The reaction mixture was stirred for ~12 h at room temperature. The samples were then centrifuged for 30 min at 13 000 rpm. The upper supernatant were recovered and continued to centrifuge for 30 min at 13 000 rpm. The upper supernatants were recovered again and added NaCl to a final concentration of 0.5 M and incubated for a few hours. Then, samples were continued to centrifuge for 5 h at 13 000 rpm. The sediments were washed with double distilled water and 2 × SSPE/0.2% SDS buffer (consisting of 2.5 mM EDTA, 7 mM SDS, 300 mM NaCl and 20 mM NaH_2PO_4 with pH 7.4) by several centrifugation cycles at 13 000 rpm in order to remove non-specifically adsorbed DNA (43,44). The samples were dispersed in 0.5 ml double distilled water and dialyzed against water for 1 day while changing water every 3 h. The molecular weight cutoff size of the dialysis membrane is 8000. Then, the sample was dialyzed one more day against sodium cacodylate buffer (100 mM NaCl, 10 mM cacodylic acid, pH 6.8). Samples were centrifuged for 30 min at 13 000 rpm, and the supernatants were collected. Thus, the SWNTs–dT_{22} conjugates were obtained.

Hybridization of dA_{22} with SWNTs–dT_{22} conjugates. Hybridization was carried out in sodium cacodylate buffer (100 mM NaCl, 10 mM cacodylic acid, pH 6.8) at 37°C for 2 h. dA_{22} was added to the SWNTs–dT_{22} solution to a final concentration of 22 μM in nucleotide. The hybridized products were designed SWNTs–dT_{22}•dA_{22} conjugates.

Coralyne induces triplex formation between SWNTs–dT_{22}•dA_{22} conjugates. Add coralyne to the SWNTs–dT_{22}•dA_{22} conjugates solution, heating to 45°C and cooling to 4°C slowly. The concentration of coralyne was 11 μM (0.5 M equivalents/bp for dT_{22} dA_{22}), and all the experiments were performed in sodium cacodylate buffer (100 mM NaCl, 10 mM cacodylic acid, pH 6.8).

Physical measurements. UV–Vis absorbance experiments were carried out on a Cary 300 UV–Vis spectrophotometer equipped with a Peltier temperature control accessory. All the spectra were measured in 1.0 cm path-length cell with the same concentration of SWNTs aqueous solution accordingly as the reference solution.

CD spectra experiments were measured on a JASCO J-810 spectropolarimeter equipped with a temperature controlled water bath. The optical chamber of CD spectrometer was deoxygenated with dry purified nitrogen

(99.99%) for 5 min at a speed of 5 l min^{-1} before use and kept the nitrogen atmosphere during experiments. Three scans were accumulated and automatically averaged. CD melting experiments of SWNTs–dT_{22}•dA_{22} conjugates in the presence of coralyne were monitored at 274 nm with a heating rate of 1.0°C min^{-1}. Primary data were transferred to the graphics program Origin for plotting and analysis.

Light scattering (LS) measurements were carried out on a JASCO FP-6500 spectrofluorometer. The LS spectra were obtained by synchronously scanning the excitation and emission monochromators of the fluorescence spectrophotometer from 250 to 700 nm (namely, $\Delta\lambda = 0$) with the slit width for the excitation and emission of 5 nm.

SEM images of DNA–SWNTs were obtained on a HITACHI S-4800 scanning electron microscope. Samples were prepared by pipetting 5 µl of colloid solution onto a silicon substrate pretreated with piranha etch solution (4:1 concentrated H_2SO_4/30% H_2O_2) for 1 h at room temperature. After evaporating the solvent, the substrate was dried overnight under vacuum.

An AFM (Nanoscope IIIa, Digital Instruments, Santa Barbara, CA, USA) was used to image SWNTs–dT_{22} or SWNTs–dT_{22}•dA_{22} conjugates in the presence or absence of coralyne. The sample solution was deposited onto a piece of freshly cleaved mica. After rinsed with water, samples were dried before measurements. Tapping mode was used to acquire the images under ambient condition.

Denaturing PAGE was used to characterize the formation of SWNTs–dT_{22} conjugate and to examine its purity. The products of reaction solution at each purifying step were loaded onto a 10% denaturing polyacrylamide gel (containing 7 M urea) using a loading buffer (30% glycerol, 25 mM EDTA, 0.01% bromophenol blue and 7 M urea). Each reaction was heated to 100°C for 3 min before loading on the gel to denature any non-specific DNA binding. The gel was run for 1 h at 100 V on a Bio-Rad vertical electrophoresis unit using TBE buffer (Tris–HCl, borate, EDTA, pH 8.0). The gels were silver-stained.

Agarose gel electrophoresis was also used to confirm the triplex formation. Electrophoresis was carried out in 0.5 % agarose gel in 0.5 × TBE (45 mM Tris, 45 mM boric acid, 1 mM EDTA, pH 8.0) as an electrophoresis buffer for 1 h at 60 V. Samples were loaded in electrophoresis buffer supplemented with glycerol to a final concentration of 20 w/v%.

RESULTS

Design of triplex-based SWNTs assembly

First, we prepared DNA–SWNTs conjugates by commonly used covalent functionalization of SWNTs with 3′-amino-modified homo-thymine ssDNA dT_{22} via carbodiimide-mediated amidation process. Then, the conjugates were hybridized with homo-adenine ssDNA dA_{22} to form SWNTs–dT_{22}•dA_{22} conjugates. The working principle in our design follows: a small molecule that can cause the strands of dA_{22}•dT_{22} to repartition into an equimolar amount of triplex dT_{22}•dA_{22}•dT_{22} and dA_{22} might lead SWNTs–dT_{22} conjugates to form a cross-linked network of nanotubes. Coralyne, a strong triplex formation inducer, should disproportionate duplex dA_{22}•dT_{22} into triplex dT_{22}•dA_{22}•dT_{22} and ss dA_{22}. Coralyne-enhanced and -directed third strand, SWNTs–dT_{22}, binding to SWNTs–dT_{22}•dA_{22} can subsequently induce SWNTs aggregation. However, when a small molecule used can not induce dT_{22}•dA_{22}•dT_{22} triplex formation, no SWNTs aggregation would occur under the same experimental conditions. Therefore, we can use this novel small molecule-directed SWNTs self-assembly assay to screen other triplex inducers. This design has been illustrated in Scheme 1.

Preparation and characterization of SWNTs–DNA conjugates

Carbodiimide-mediated amidations of SWNTs is a common method that was widely used to prepare DNA or protein–SWNTs conjugates (16,43,45,46). Oxidized SWNTs (0.1 mg ml^{-1}) and ssDNA (2 µM) solutions were mixed in the presence of EDC (20 mM) and Sulfo-NHS (20 mM), then incubated for 12 h. After separation and purification steps, the soluble fraction obtained from coupling to $(dT)_{22}$–NH_2 consists of a clear, transparent, blackish, homogeneous suspension as shown in Figure 1a. Denaturing PAGE and UV–Vis spectroscopy were used to characterize the purified SWNTs–$(dT)_{22}$ conjugates. After the sample was dialyzed and centrifuged as described in the materials section, dT_{22} alone was not observed (Figure 1b, lane 2). Since the average length of SWNT is about several hundred nanometers long, the major SWNT–DNA conjugate hardly moved in denatured PAGE although the short SWNT-formed DNA conjugate may run faster than the long-SWNT–DNA conjugate. These results suggest that we obtained purified SWNT–DNA conjugates. Compared the UV–Vis spectra of SWNTs–dT_{22} conjugates with SWNTs alone, there is an apparent peak ~260 nm in the UV–Vis spectrum of SWNT–dT_{22} conjugates, while no peaks at this range existed in the UV–Vis spectrum of SWNTs alone that clearly indicate that DNA molecules have been successfully attached to SWNTs (Figure 1c). Scanning electron microscopy (SEM) and atomic force microscopy (AFM) images (Figure 1d and e) also confirm the conjugation of ssDNA with SWNTs.

Then, SWNTs–dT_{22} was hybridized with its complementary strand, dA_{22} (22 µM in nucleotide) to form duplex in sodium cacodylate buffer (100 mM NaCl, 10 mM cacodylic acid, pH 6.8) at 37°C. After separation and purification, the SWNTs–dT_{22}•dA_{22} conjugates were characterized by circular dichroism (CD) spectroscopy (Figure 2a). CD spectrum of SWNTs-conjugated dA_{22}•dT_{22} sample is similar to duplex dA_{22}•dT_{22} alone. Figure 2b shows that SWNTs-conjugated dA_{22}•dT_{22} has an apparent melting transition at 46.7°C observed in its melting curve, indicating that SWNTs–dT_{22} forms duplex in the presence of dA_{22}.

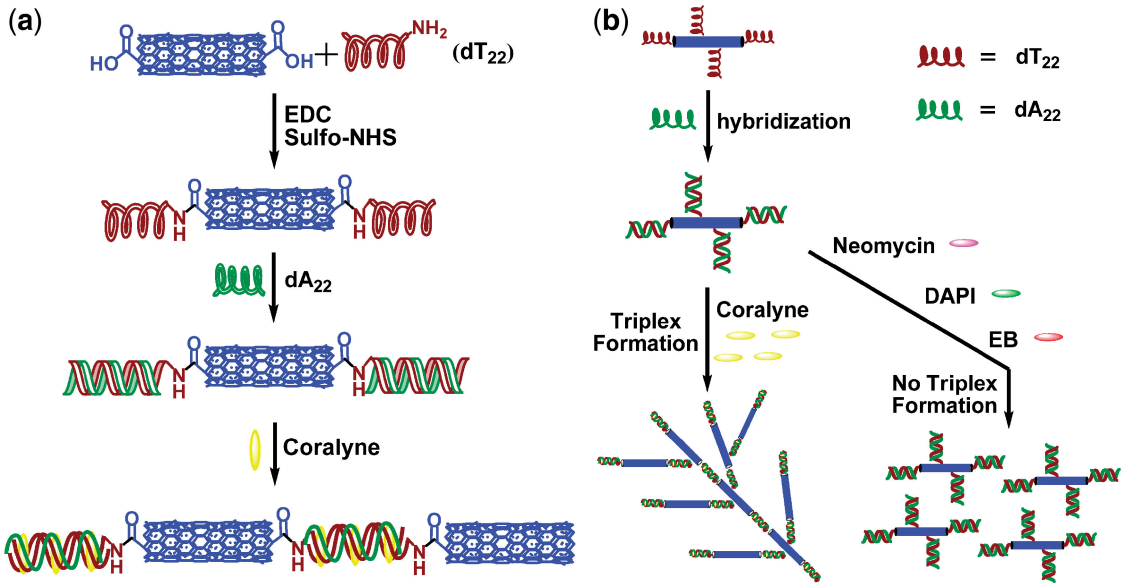

Scheme 1. (**a**) Schematic representation of the fabrication of DNA–SWNTs conjugates and coralyne induced self-assembly of SWNTs based on triplex formation. (**b**) SWNTs-assembled nanostructure directed by coralyne-induced triplex formation and this assay used for screening of triplex inducers. Small molecules used are typical DNA binders, including neomycin, EB and DAPI.

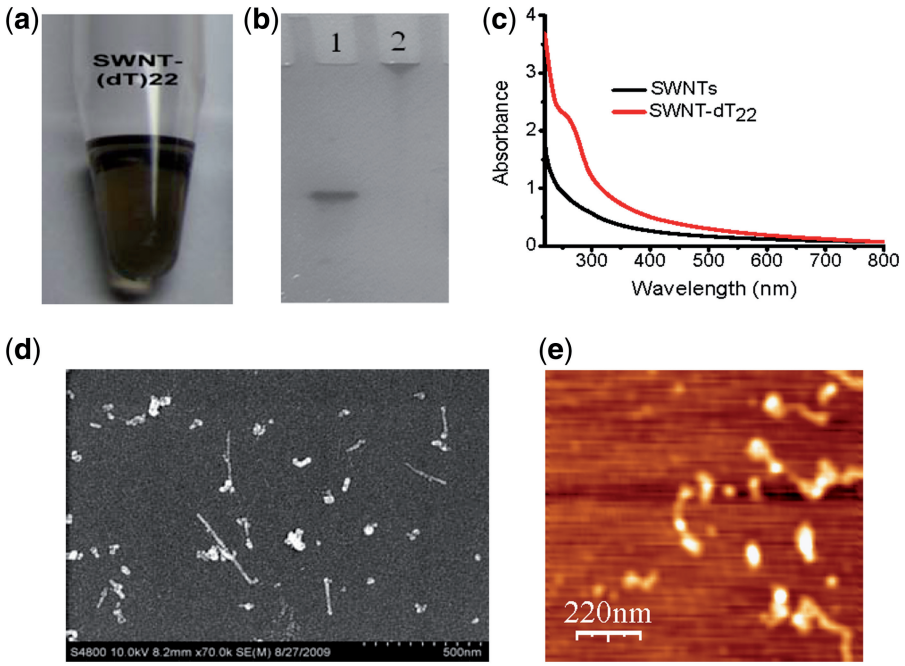

Figure 1. Characterization of SWNTs–dT_{22} conjugates. (**a**) Photograph of the supernatant fraction obtained from the coupling steps with dT_{22}. (**b**) Denaturing PAGE image of (lane 1) dT_{22} alone; (lane 2) purified SWNTs–dT_{22} conjugates. (**c**) UV–Vis absorption spectra of SWNTs (black line) and SWNTs–dT_{22} conjugates (red line); (**d**) SEM image of SWNTs–dT_{22} conjugates. After the sample was purified as described in 'Materials and Methods' section, SEM shows that SWNTs are dispersed upon DNA conjugation. (**e**) AFM image of SWNTs–dT_{22} conjugates. AFM indicates that dT_{22} are conjugated to SWNTs and the formed conjugates are dispersed.

Coralyne directed self-assembling of SWNTs and screening of triplex inducers

The coralyne-directed SWNTs self-assembling was accomplished by adding coralyne (11 μM, 0.5 M equivalents/base pair for dT_{22}•dA_{22}) to the SWNTs–dT_{22}•dA_{22} conjugates in sodium cacodylate buffer (100 mM NaCl, 10 mM cacodylic acid, pH 6.8), and then the sample was heated to 45°C and cooled to 4°C slowly. The solution was then analyzed by LS spectroscopy. In the absence of coralyne, LS spectra of SWNTs–dT_{22}•dA_{22} conjugates (Figure 3a, black and blue lines) did not show significant difference

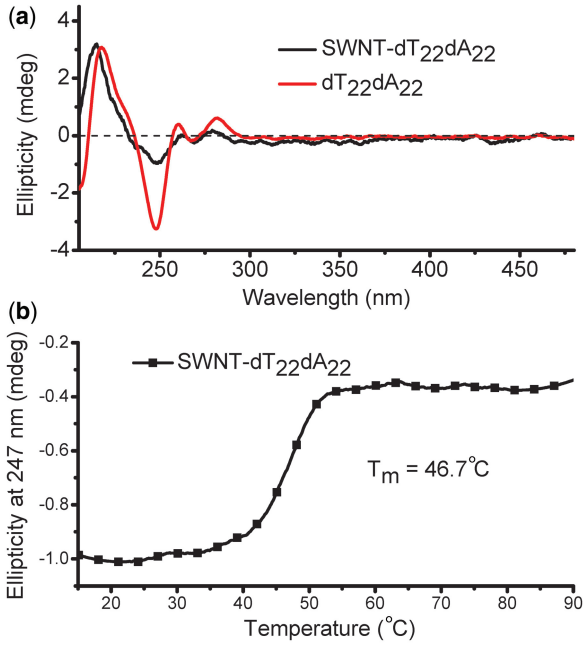

Figure 2. (**a**) CD spectra of the duplex dA_{22}•dT_{22} (red line) and SWNTs–dT_{22}•dA_{22} conjugates (black line). (**b**) CD melting profile of the SWNTs–dT_{22}•dA_{22} conjugates.

before and after heating, that indicates that aggregation does not occur. However, in the presence of coralyne, the LS intensity at 555 nm (Figure 3a, red line) increases remarkably, suggesting that the coralyne induced triplex formation and caused SWNTs aggregation. In contrast, this change can not be observed for a random selected DNA sequence (control DNA: 5′-CCA ACC CCC CAG AAA GAA-3′), that was used instead of dA_{22} to hybridize with SWNTs–dT_{22} conjugates under the same conditions (Figure 3b). To go further, we decide to explore if this assay can be used to screen triplex inducers. Typical duplex binders (chemical structures are shown in Scheme 2) are used in this assay. Ethidium bromide (EB; a typical DNA intercalator) and 4′,6-diamidino-2-phenylindole (DAPI; a typical minor groove binder) were tested using SWNTs–dT_{22}•dA_{22} conjugates under the same experimental conditions, no intensity change was observed in their LS spectra (Figure 3c). Neomycin, a typical major groove binder, has been recently reported as a triplex stabilizing compound (47,48). However, due to its weak inducing capability (Supplementary Figure S1), neomycin can not drive SWNTs–dT_{22}•dA_{22} to form triplex under the same coralyne experimental conditions and no LS signal change was observed either (Figure 3c). These results indicate that this novel small molecule-directed SWNTs self-assembly assay can also be used for screening of triplex inducers. The control experiments using random sequence and none triplex formation inducers confirm that the observed spectral change is due to coralyne-directed third strand SWNTs–dT_{22} binding to SWNTs–dT_{22}•dA_{22} that subsequently induces SWNTs aggregation. This is further supported by our next CD, SEM, AFM and electrophoresis results.

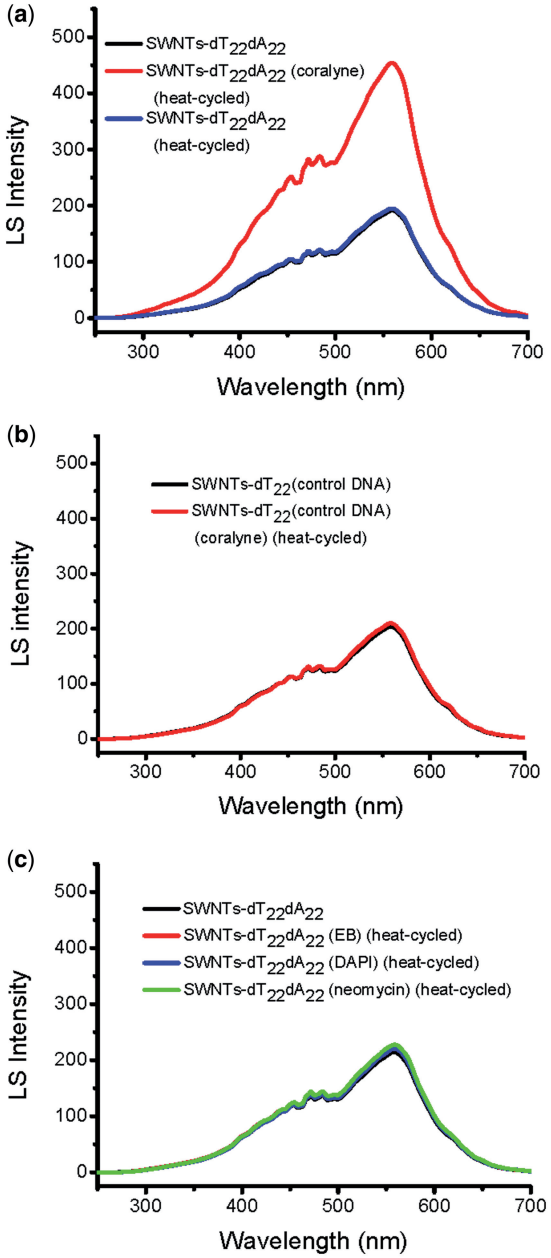

Figure 3. LS spectra of the SWNTs–DNA conjugates under different conditions. (**a**) SWNTs–dT_{22}•dA_{22} conjugates in the absence or presence of coralyne. (**b**) SWNTs–dT_{22} with control DNA (random sequence) conjugates in the absence or presence of coralyne. (**c**) SWNTs–dT_{22}•dA_{22} conjugates in the absence or presence of different DNA binders: EB, DAPI and neomycin.

Demonstration of triplex formation

CD spectroscopy was used to monitor coralyne-induced conformational change of duplex dA_{22}•dT_{22} and SWNTs–dT_{22}•dA_{22}.

Coralyne can cause disproportionation of duplex dA_{22}•dT_{22} at 45°C. The CD spectrum of duplex dA_{22}•dT_{22} at 4°C changes dramatically upon the addition of 0.5 M equivalents of coralyne per DNA base pair (Supplementary Figure S2a). These changes include the appearance of a

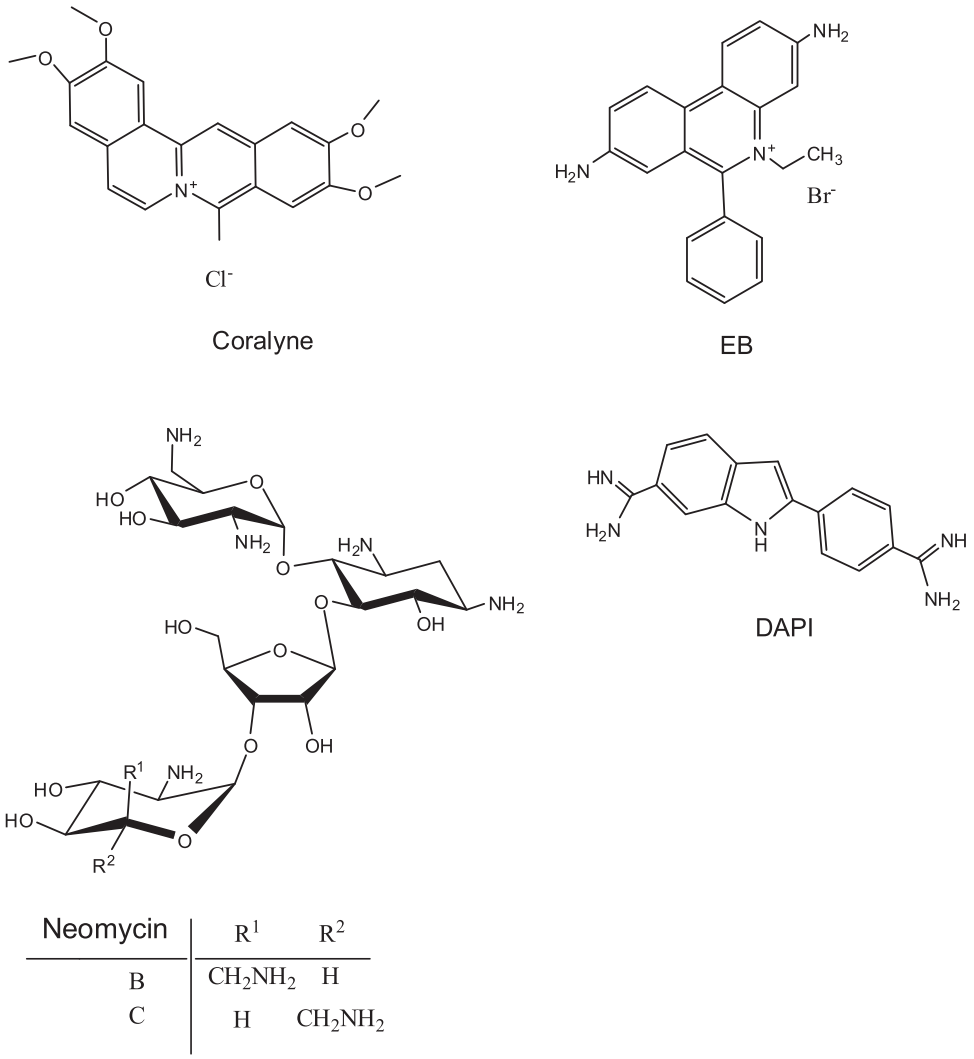

Scheme 2. Chemical structures of coralyne, EB, DAPI and neomycin.

substantial positive CD bands near 300 nm and negative CD bands near 350 nm. However, typical CD bands of triplex DNA with intercalated coralyne at ~340 and ~440 nm are virtually non-existed (36,37,48). This indicates that coralyne does not cause the complete and spontaneous formation of triplex DNA at 4°C.

Heating of $dA_{22}\cdot dT_{22}$ sample with added coralyne to 45°C dramatically reduces the magnitude of the duplex-specific coralyne CD bands at 300 and 350 nm (Supplementary Figure S2b); small positive bands at ~340 and ~440 nm (Supplementary Figure S2b) are observed, similar to CD bands observed for coralyne intercalated in the $dT_{22}\cdot dA_{22}\cdot dT_{22}$ triplex (Supplementary Figure S2d). Additionally, the melting profile of the $dA_{22}\cdot dT_{22}$ sample in the presence of coralyne exhibits a transition at 66.1°C (Supplementary Figure S3a), which shows the same transition temperature of coralyne-intercalated triplex $dT_{22}\cdot dA_{22}\cdot dT_{22}$ (Supplementary Figure S3b). The magnitude of this transition in the CD melting profile of the duplex sample with added coralyne is half the transition in the triplex sample with added coralyne (Supplementary Figure S3a and b), which is also consistent with the $dA_{22}\cdot dT_{22}$ sample being disproportioned by coralyne into 0.5 M equivalents of triplex $dT_{22}\cdot dA_{22}\cdot dT_{22}$ and 0.5 M equivalents of dA_{22}. Thus, the 66.1°C transition in the $dA_{22}\cdot dT_{22}$ sample with coralyne can be assigned to the melting of coralyne-intercalated triplex $dT_{22}\cdot dA_{22}\cdot dT_{22}$ in the disproportioned sample.

The process of duplex disproportionation by coralyne in the $dA_{22}\cdot dT_{22}$ sample during the first time heating has broad transition (Supplementary Figure S3a), showing that coralyne-induced duplex disproportionation is cooperative. The central transition is at 39.5°C (Supplementary Figure S3a). During the second time heating of the same sample, this broad transition is absent (Supplementary Figure S3a). This indicates that the intercalated triplex and dA_{22} of a coralyne-disproportioned duplex sample do not immediately revert back to the duplex state when the sample is returned to 4°C. This lack of reversion from the disproportioned state is also supported by the fact that the CD

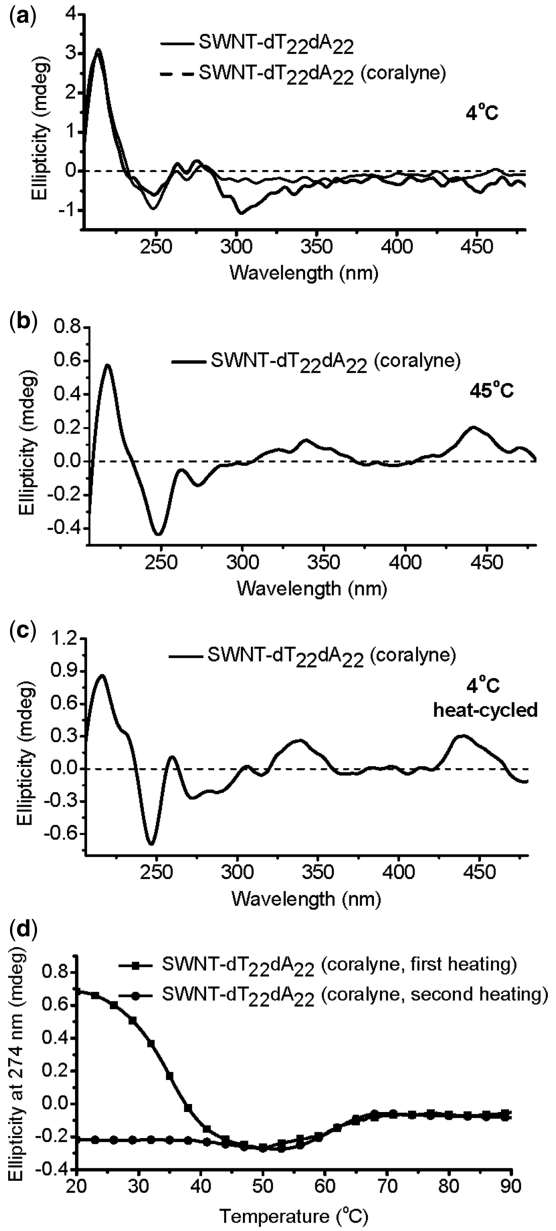

Figure 4. CD spectra of SWNTs–dT_{22}•dA_{22}. (**a**) SWNTs–dT_{22}•dA_{22} in the absence or presence of coralyne at 4°C prior to heating. (**b**) Spectra of SWNTs–dT_{22}•dA_{22} in the presence of coralyne at 45°C. (**c**) Heat-cycled spectrum of disproportioned SWNTs–dT_{22}•dA_{22} sample in the presence of coralyne at 4°C. (**d**) CD melting profiles for SWNTs–dT_{22}•dA_{22} samples at 274 nm to show structural transitions: first time (black line) and second time heating (red line) of SWNTs–dT_{22}•dA_{22} after the addition of coralyne.

spectrum of the coralyne-disproportioned dA_{22}•dT_{22} at 4°C after heat cycling (from 4°C to 80°C and back to 4°C) is radically different from the CD spectrum of the sample prior to heating (Supplementary Figure S2a and c). Furthermore, there is an excellent match between the CD spectrum of coralyne-disproportioned dA_{22}•dT_{22} sample and a composite CD spectrum generated by the summation of a CD spectrum of coralyne-intercalated triplex dT_{22}•dA_{22}•dT_{22} and the CD spectrum of dA_{22} in the presence of coralyne (Supplementary Figure S2c).

Coralyne can also cause disproportionation of duplex SWNTs–dT_{22}•dA_{22} at 45°C. As shown in Figure 4a, coralyne can not cause duplex SWNTs–dT_{22}•dA_{22} to form triplex at 4°C (the same CD spectrum characteristics with that of dA_{22}•dT_{22}/coralyne (Supplementary Figure S2). However, heating SWNTs–dT_{22}•dA_{22} sample with added coralyne to 45°C, CD spectrum shows typical features of DNA triplex with intercalated coralyne, together with appearance of small positive CD bands at ~340 and ~440 nm (Figure 4b) (36,37,49), similar to the case of dA_{22}•dT_{22}/coralyne in the absence of SWNTs (Supplementary Figure S2). After cooling to 4°C, the CD spectrum is significantly different from that of the same sample at 4°C prior to being heated (Figure 4a and c), showing that the transition to a sample of complete coralyne-intercalated triplex is not reversed upon cooling. This is also illustrated by the fact that the CD melting profile for the first heating of the SWNTs–dT_{22}•dA_{22} sample with coralyne has a transition at ~35°C, that is assigned to DNA strand reorganization (36,37). That transition is disappeared during the second heating of the sample and one single transition at ~61°C is observed, that is attributed to the intercalated triplex melts into single strands (Figure 4d).

Morphology of dA_{22}•dT_{22}–SWNTs–coralyne assembly

To directly study the morphology of dA_{22}•dT_{22}–SWNTs–coralyne assemblies, we deposited a mixture of dA_{22}•dT_{22}–SWNTs and coralyne on a silicon substrate and observed the aggregates (Figure 5) by SEM and AFM (40,43). As shown in Figure 5a, in the presence of coralyne, SEM results clearly show that the aggregates form large DNA-linked 3D nanostructure. The SWNTs are linked to each other due to the triplex dT_{22}•dA_{22}•dT_{22} formation via bound coralyne (Figure 5b), however, this is not observed for dA_{22}•dT_{22}–SWNTs conjugates in the absence of coralyne (Figure 5c). AFM images also support that the SWNTs are cross-linked and form large nanostructure in the presence of coralyne (Figure 5d). Electrophoretic mobility shift assay (41,43,50) was also used to compare the size between coralyne-induced SWNTs aggregates and SWNTs–dT_{22}•dA_{22} duplex (Supplementary Figure S4). In combination with CD, LS spectroscopy, gel mobility shift, SEM and AFM results, coralyne can induce triplex formation and cause SWNTs cross-linked and form large assembly.

DISCUSSION

Self-assembly has received much attention aimed at integrating nanoscale building blocks into functioning devices. SWNTs have already been considered as 'building blocks' in nano/microelectronic devices. However, since SWNTs lack chemical recognition, SWNT-based electronic devices and sensors are strictly related to the development of a bottom-up self-assembly technique. The specific molecular recognition of DNA coupled with SWNTs and the hybridization of these macromolecular wires make the DNA molecule an ideal

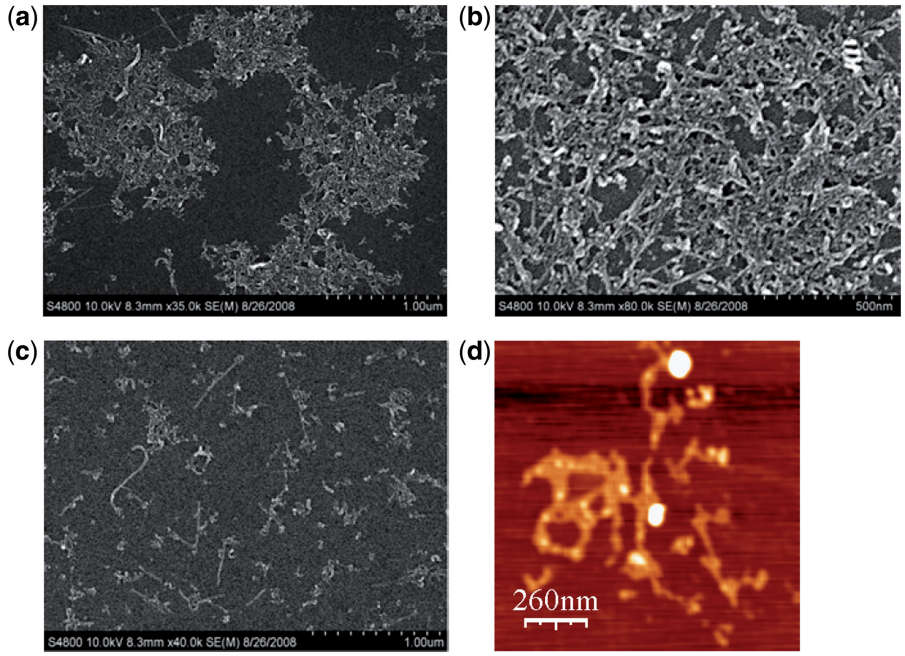

Figure 5. (**a** and **b**) SEM images of heat-cycled SWNTs–dT_{22}•dA_{22} in the presence of coralyne. (**c**) SEM image of heat-cycled SWNTs–dT_{22}•dA_{22} without coralyne. (**d**) AFM image of heat-cycled SWNTs–dT_{22}•dA_{22} sample in the presence of coralyne.

candidate for this task. Here we report for the first time that a small triplex formation inducer (coralyne) can cause the self-assembly of SWNTs by disproportionation of duplex DNA into triplex and ssDNA.

Coralyne, a small crescent-shaped molecule, can intercalate into both duplex and triplex DNA, but binds stronger to triplex DNA (51–55). Polak and Hud have demonstrated that coralyne can cause complete and irreversible disproportionation of duplex poly(dT)•poly(dA) into a 1:1 mixture of coralyne-intercalated triplex poly(dT)•poly(dA)•poly(dT) and poly(dA), with each resulting structure being at one half the concentration of the original duplex (37,38). We have also observed that coralyne can cause duplex dA_{22}•dT_{22} to repartition into a 1:1 mixture of coralyne-intercalated triplex dT_{22}•dA_{22}•dT_{22} and dA_{22}. CD spectra and melting experiments indicate that this unique property of coralyne is also applicable to the duplex dA_{22}•dT_{22} that is attached to the surface of SWNTs. This is intriguing not only for its property, but also for its application to the controllable self-assembly of SWNTs. Coralyne can cross-link two separate SWNTs–dT_{22}•dA_{22} conjugates by forming a coralyne-intercalated triplex SWNT–dT_{22}•dA_{22}•dT_{22}–SWNT and dA_{22}, that leads to SWNTs aggregation and forms large DNA-linked 3D nanostructure (Scheme 1). This has been studied by using LS spectroscopy, SEM, AFM and electrophoretic mobility shift assay.

In order to further verify our design principle, we also used other DNA duplex binders to see whether these small molecules can direct SWNTs self-assembly. EB can intercalate into DNA. DAPI is a fluorescent dye that can bind strongly to DNA. Two DNA-binding modes have been suggested for DAPI: one is minor groove-binding mode, preferentially interacting with AT-rich regions (56,57); the other is intercalation into GC or mixed GC and AT DNA sequences (58–60). Neomycin is one of the most effective aminoglycoside groove binders to stabilize DNA triple helix. Neomycin selectively stabilizes triplex DNA and hardly influence duplex DNA (47,48). Under the same coralyne experimental conditions, all these small molecules can not drive dT_{22}•dA_{22} to form triplex. These results indicate that although neomycin can enhance triplex DNA stability it can not induce duplex dT_{22}•dA_{22} disproportionation to form triplex dT_{22}•dA_{22}•dT_{22} (Figure 3 and Supplementary Figure S1), neomycin is a triplex DNA stabilizer but not an effective triplex inducer.

CONCLUSION

In summary, DNA triplex formation has been considered a promising strategy for realizing artificially control of gene expression, reversible assembly of nanomaterials and DNA nanomachine. Here we design a small molecule-directed SWNTs self-assembly assay by disproportionation of duplex into triplex by triplex formation inducer, coralyne. This design has been studied by CD, LS spectroscopy, SEM, AFM, electrophoretic mobility shift assay and supported by using DNA random sequence. For small molecules that can not induce triplex formation, SWNTs do not aggregate under the same experimental conditions. Besides, specific small molecule-fueled cross-linking of SWNTs networks can be useful in the area of nanobiotechnology. For example, this small molecule-directed SWNTs assembling can offer a potential method to facilitate construction of

desired SWNTs nanoscale multicomponent/multifunctional architectures for electrical and biosensing applications.

SUPPLEMENTARY DATA

Supplementary Data are available at NAR Online.

FUNDING

973 Project 2011CB936004; NSFC (20831003, 90813001, 20833006, 90913007); Chinese Academy of Sciences. Funding for open access charge: NSFC; 973 Project.

Conflict of interest statement. None declared.

REFERENCES

1. Dresselhaus,M.S., Dresselhaus,G. and Eklund,P.C. (1996) *Science of Fullerenes and Carbon Nanotubes*. Academic Press, San Diego, pp. 1–985.
2. Tasis,D., Tagmatarchis,N., Bianco,A. and Prato,M. (2006) Chemistry of carbon nanotubes. *Chem. Rev.*, **106**, 1105–1136.
3. Britz,D.A. and Khlobystov,A.N. (2006) Noncovalent interactions of molecules with single walled carbon nanotubes. *Chem. Soc. Rev.*, **35**, 637–659.
4. Valcarcel,M., Cardenas,S. and Simonet,B.M. (2007) Role of carbon nanotubes in analytical science. *Anal. Chem.*, **79**, 4788–4797.
5. Postma,H.W., Teepen,T., Yao,Z., Grifoni,M. and Dekker,C. (2001) Carbon nanotube single-electron transistors at room temperature. *Science*, **293**, 76–79.
6. Tans,S.J., Verschueren,A.R.M. and Dekker,C. (1998) Room-temperature transistor based on a single carbon nanotube. *Nature*, **393**, 49–52.
7. Bachtold,A., Hadley,P., Nakanishi,T. and Dekker,C. (2001) Logic circuits with carbon nanotube transistors. *Science*, **294**, 1317–1320.
8. Javey,A., Wang,Q., Ural,A., Li,Y.M. and Dai,H.J. (2002) Carbon nanotube transistor arrays for multistage complementary logic and ring oscillators. *Nano Lett.*, **2**, 929–932.
9. Heath,J.R. and Ratner,M.A. (2003) Molecular electronics. *Phys. Today*, **56**, 43–49.
10. Lund,K., Manzo,A.J., Dabby,N., Michelotti,N., Johnson-Buck,A., Nangreave,J., Taylor,S., Pei,R., Stojanovic,M.N., Walter,N.G. *et al*. (2010) Molecular robots guided by prescriptive landscapes. *Nature*, **465**, 206–210.
11. Zheng,J., Birktoft,J.J., Chen,Y., Wang,T., Sha,R., Constantinou,P.E., Ginell,S.L., Mao,C. and Seeman,N.C. (2009) From molecular to macroscopic via the rational design of a self-assembled 3D DNA crystal. *Nature*, **461**, 74–77.
12. Keren,K., Krueger,M., Gilad,R., Ben-Yoseph,G., Sivan,U. and Braun,E. (2002) Sequence-specific molecular lithography on single DNA molecules. *Science*, **297**, 72–75.
13. Wang,X., Liu,F., Andavan,G.T., Jing,X., Singh,K., Yazdanpanah,V.R., Bruque,N., Pandey,R.R., Lake,R., Ozkan,M. *et al*. (2006) Carbon nanotube-DNA nanoarchitectures and electronic functionality. *Small*, **2**, 1356–1365.
14. Katz,E. and Willner,I. (2004) Biomolecule-functionalized carbon nanotubes: applications in nanobioelectronics. *Chemphyschem*, **5**, 1084–1104.
15. Dwyer,C., Guthold,M., Falvo,M., Washburn,S., Superfine,R. and Erie,D. (2002) DNA-functionalized single-walled carbon nanotubes. *Nanotechnology*, **13**, 601–604.
16. Hazani,M., Naaman,R., Hennrich,F. and Kappes,M.M. (2003) Confocal fluorescence imaging of DNA-functionalized carbon nanotubes. *Nano Lett.*, **3**, 153–155.
17. Zheng,M., Jagota,A., Semke,E.D., Diner,B.A., McLean,R.S., Lustig,S.R., Richardson,R.E. and Tassi,N.G. (2003) DNA-assisted dispersion and separation of carbon nanotubes. *Nat. Mater.*, **2**, 338–342.
18. Singh,R., Pantarotto,D., McCarthy,D., Chaloin,O., Hoebeke,J., Partidos,C.D., Briand,J.P., Prato,M., Bianco,A. and Kostarelos,K. (2005) Binding and condensation of plasmid DNA onto functionalized carbon nanotubes: toward the construction of nanotube-based gene delivery vectors. *J. Am. Chem. Soc.*, **127**, 4388–4396.
19. Li,S., He,P., Dong,J., Guo,Z. and Dai,L. (2005) DNA-directed self-assembling of carbon nanotubes. *J. Am. Chem. Soc.*, **127**, 14–15.
20. Hazani,M., Hennrich,F., Kappes,M., Naaman,R., Peled,D., Sidorov,V. and Shvarts,D. (2004) DNA-mediated self-assembly of carbon nanotube-based electronic devices. *Chem. Phys. Lett.*, **391**, 389–392.
21. Lu,Y.H., Yang,X.Y., Ma,Y.F., Du,F., Liu,Z.F. and Chen,Y.S. (2006) Self-assembled branched nanostructures of single-walled carbon nanotubes with DNA as linkers. *Chem. Phys. Lett.*, **419**, 390–393.
22. Li,Y.L., Han,X.G. and Deng,Z.X. (2007) Grafting single-walled carbon nanotubes with highly hybridizable DNA sequences: potential building blocks for DNA-programmed material assembly. *Angew. Chem. Int. Ed.*, **46**, 7481–7484.
23. Feng,L., Li,X., Peng,Y., Geng,J., Ren,J. and Qu,X. (2009) Spectral and electrochemical detection of protonated triplex formation by a small-molecule anticancer agent. *Chem. Phys. Lett.*, **480**, 309–312.
24. Helene,C. (1991) The anti-gene strategy: control of gene expression by triplex-forming-oligonucleotides. *Anticancer Drug Des.*, **6**, 569–584.
25. Maher,L.J. 3rd (1992) DNA triple-helix formation: an approach to artificial gene repressors? *Bioessays*, **14**, 807–815.
26. Duval-Valentin,G., de Bizemont,T., Takasugi,M., Mergny,J.L., Bisagni,E. and Helene,C. (1995) Triple-helix specific ligands stabilize H-DNA conformation. *J. Mol. Biol.*, **247**, 847–858.
27. Maher,L.J. 3rd (1996) Prospects for the therapeutic use of antigene oligonucleotides. *Cancer Invest.*, **14**, 66–82.
28. Jung,Y.H., Lee,K.B., Kim,Y.G. and Choi,I.S. (2006) Proton-fueled, reversible assembly of gold nanoparticles by controlled triplex formation. *Angew. Chem. Int. Ed.*, **45**, 5960–5963.
29. Han,M.S., Lytton-Jean,A.K. and Mirkin,C.A. (2006) A gold nanoparticle based approach for screening triplex DNA binders. *J. Am. Chem. Soc.*, **128**, 4954–4955.
30. Helene,C. (1998) DNA recognition. Reading the minor groove. *Nature*, **391**, 436–438.
31. Chan,P.P. and Glazer,P.M. (1997) Triplex DNA: fundamentals, advances, and potential applications for gene therapy. *J. Mol. Med.*, **75**, 267–282.
32. Faria,M. and Giovannangeli,C. (2001) Triplex-forming molecules: from concepts to applications. *J. Gene Med.*, **3**, 299–310.
33. Niemeyer,C.M. (2000) Self-assembled nanostructures based on DNA: towards the development of nanobiotechnology. *Curr. Opin. Chem. Biol.*, **4**, 609–618.
34. Brucale,M., Zuccheri,G. and Samori,B. (2005) The dynamic properties of an intramolecular transition from DNA duplex to cytosine-thymine motif triplex. *Org. Biomol. Chem.*, **3**, 575–577.
35. Plum,G.E. (1997) Thermodynamics of oligonucleotide triple helices. *Biopolymers*, **44**, 241–256.
36. Xing,F., Song,G., Ren,J., Chaires,J.B. and Qu,X. (2005) Molecular recognition of nucleic acids: coralyne binds strongly to poly(A). *FEBS Lett.*, **579**, 5035–5039.
37. Polak,M. and Hud,N.V. (2002) Complete disproportionation of duplex poly(dT)•poly(dA) into triplex poly(dT)•poly(dA) •poly(dT) and poly(dA) by coralyne. *Nucleic Acids Res.*, **30**, 983–992.
38. Persil,O., Santai,C.T., Jain,S.S. and Hud,N.V. (2004) Assembly of an antiparallel homo-adenine DNA duplex by small-molecule binding. *J. Am. Chem. Soc.*, **126**, 8644–8645.
39. Li,X., Peng,Y., Ren,J. and Qu,X. (2006) Carboxyl-modified single-walled carbon nanotubes selectively induce human telomeric i-motif formation. *Proc. Natl Acad. Sci. USA*, **103**, 19658–19663.

40. Li,X., Peng,Y. and Qu,X. (2006) Carbon nanotubes selective destabilization of duplex and triplex DNA and inducing B-A transition in solution. *Nucleic Acids Res.*, **34**, 3670–3676.
41. Zhao,C., Ren,J. and Qu,X. (2008) Single-walled carbon nanotubes binding to human telomeric i-motif DNA under molecular-crowding conditions: more water molecules released. *Chem. Eur. J.*, **14**, 5435–5439.
42. Zhao,C., Peng,Y., Song,Y., Ren,J. and Qu,X. (2008) Self-assembly of single-stranded RNA on carbon nanotube: polyadenylic acid to form a duplex structure. *Small*, **4**, 656–661.
43. Zhao,C., Song,Y., Ren,J. and Qu,X. (2009) A DNA nanomachine induced by single-walled carbon nanotubes on gold surface. *Biomaterials*, **30**, 1739–1745.
44. Baker,S.E., Cai,W., Lasseter,T.L., Weidkamp,K.P. and Hamers,R.J. (2002) Covalently bonded adducts of deoxyribonucleic acid (DNA) oligonucleotides with single-wall carbon nanotubes: Synthesis and hybridization. *Nano Lett.*, **2**, 1413–1417.
45. Wong,S.S., Woolley,A.T., Joselevich,E., Cheung,C.L. and Lieber,C.M. (1998) Covalently-functionalized single-walled carbon nanotube probe tips for chemical force microscopy. *J. Am. Chem. Soc.*, **120**, 8557–8558.
46. Huang,W.J., Taylor,S., Fu,K.F., Lin,Y., Zhang,D.H., Hanks,T.W., Rao,A.M. and Sun,Y.P. (2002) Attaching proteins to carbon nanotubes via diimide-activated amidation. *Nano Lett.*, **2**, 311–314.
47. Arya,D.P., Coffee,R.L. Jr, Willis,B. and Abramovitch,A.I. (2001) Aminoglycoside-nucleic acid interactions: remarkable stabilization of DNA and RNA triple helices by neomycin. *J. Am. Chem. Soc.*, **123**, 5385–5395.
48. Arya,D.P., Micovic,L., Charles,I., Coffee,R.L. Jr, Willis,B. and Xue,L. (2003) Neomycin Binding to Watson-Hoogsteen (W-H) DNA Triplex Groove: a Model. *J. Am. Chem. Soc.*, **125**, 3733–3744.
49. Jain,S.S., Polak,M. and Hud,N.V. (2003) Controlling nucleic acid secondary structure by intercalation: effects of DNA strand length on coralyne-driven duplex disproportionation. *Nucleic Acids Res.*, **31**, 4608–4615.
50. Vetcher,A.A., Srinivasan,S., Vetcher,I.A., Abramov,S.M., Kozlov,M., Baughman,R.H. and Levene,S.D. (2006) Fractionation of SWNT/nucleic acid complexes by agarose gel electrophoresis. *Nanotechnology*, **17**, 4263–4269.
51. Lee,J.S., Latimer,L.J.P. and Hampel,K.J. (1993) Coralyne binds tightly to both T•A•T-containing and C•G•C^+-containing DNA triplexes. *Biochemistry*, **32**, 5591–5597.
52. Wilson,W.D., Tanious,F.A., Mizan,S., Yao,S.J., Kiselyov,A.S., Zon,G. and Strekowski,L. (1993) DNA triple-helix specific intercalators as antigene enhancers: unfused aromatic cations. *Biochemistry*, **32**, 10614–10621.
53. Wilson,W.D., Mizan,S., Tanious,F.A., Yao,S. and Zon,G. (1994) The interaction of intercalators and groove-binding agents with DNA triple-helical structures: the influence of ligand structure, DNA backbone modifications and sequence. *J. Mol. Recogit.*, **7**, 89–98.
54. Latimer,L.J.P., Payton,N., Forsyth,G. and Lee,J.S. (1995) The binding of analogs of coralyne and related heterocyclics to DNA triplexes. *Biochem. Cell Biol.*, **73**, 11–18.
55. Ren,J.S. and Chaires,J.B. (1999) Sequence and structural selectivity of nucleic acid binding ligands. *Biochemistry*, **38**, 16067–16075.
56. Larsen,T.A., Goodsell,D.S., Cascio,D., Grzeskowiak,K. and Dickerson,R.E. (1989) The structure of DAPI bound to DNA. *J. Biomol. Struct. Dyn.*, **7**, 477–491.
57. Tanious,F.A., Veal,J.M., Buczak,H., Ratmeyer,L.S. and Wilson,W.D. (1992) DAPI (4′,6-diamidino-2-phenylindole) binds differently to DNA and RNA: minor-groove binding at AT sites and intercalation at AU sites. *Biochemistry*, **31**, 3103–3112.
58. Wilson,W.D., Tanious,F.A., Barton,H.J., Jones,R.L., Fox,K.R., Wydra,R.L. and Strekowski,L. (1990) DNA sequence dependent binding modes of 4′,6-diamidino-2-phenylindole (DAPI). *Biochemistry*, **29**, 8452–8461.
59. Kim,S.K., Eriksson,S., Kubista,M. and Norden,B. (1993) Interaction of 4′,6-diamidino-2-phenylindole (DAPI) with poly[d(G-C)$_2$] and poly[d(G-m^{5}C)$_2$]: evidence for major groove binding of a DNA probe. *J. Am. Chem. Soc.*, **115**, 3441–3447.
60. Sehlstedt,U., Kim,S.K. and Norden,B. (1993) Binding of 4′,6-diamidino-2-phenylindole to [poly(dI-dC)]$_2$ and [poly(dG-dC)]$_2$: the exocyclic amino group of guanine prevents minor groove binding. *J. Am. Chem. Soc.*, **115**, 12258–12263.